K+ Efflux Is Required for Histone H3 Dephosphorylation by *Listeria monocytogenes* Listeriolysin O and Other Pore-Forming Toxins[∇]

Mélanie Anne Hamon and Pascale Cossart*

Institut Pasteur, Unité des Interactions Bactéries-Cellules, Paris F-75015, France; INSERM, U604, Paris F-75015, France; and INRA, USC2020, Paris F-75015, France

Chromatin modification triggered by bacteria is a newly described mechanism by which pathogens impact host transcription. *Listeria monocytogenes* dephosphorylates histone H3 through the action of listeriolysin O (LLO); however, the underlying mechanism is unknown. Here we show that an unrelated pore-forming toxin, *Aeromonas* aerolysin, also provokes H3 dephosphorylation (dePH3). As reported for aerolysin, we show that LLO and related toxins induce a pore-dependent K+ efflux and that this efflux is the signal required for dePH3. In addition, LLO-induced K+ efflux activates caspase-1. However, we demonstrate that dePH3 is unlinked to this activation. Therefore, our study unveils K+ efflux as an important signal leading to two independent events critical for infection, inflammasome activation and histone modification.

Posttranslational modification of histone tails is a mechanism originally observed during viral infections and recently reported for several bacterial pathogens (12). Histones are essential players in eukaryotic chromatin formation, contributing to the packaging of DNA in the nucleus while retaining the properties of DNA for replication, transcription, etc. Chromatin is composed of an octameric complex of histones H2A, H2B, H3, and H4 around which DNA wraps and condenses into a nucleosome. It is now clear that modifications of N-terminal histone tails induce changes in chromatin and control access of the transcriptional machinery to promoter regions, thereby regulating gene expression. To date, a few bacteria have been shown to modulate host chromatin. However, the underlying mechanisms remain unknown (2, 12).

Listeria monocytogenes is an invasive pathogen which secretes a pore-forming toxin, listeriolysin O (LLO), during infection. LLO is part of a large family of cholesterol-dependent cytolysins (CDCs), all produced by Gram-positive bacteria (4, 24). *L. monocytogenes* and the closely related species *Listeria ivanovii* are the only intracellular bacteria to produce such a toxin. However, secretion of LLO is not restricted to the intracellular compartment and can also occur outside cells (14, 28). The pores formed by CDCs are large (25 to 30 nm), and except for one member (9), CDCs have no known protein receptors, although cholesterol is a prerequisite for pore formation. LLO and other CDCs are potent signaling molecules triggering a variety of cellular responses, including mitogen-activated protein kinase and NF-κB activation, Ca2+ signaling, and lipid raft aggregation (28). In addition, we have shown that LLO and CDCs provoke several histone modifications (11). However, the underlying mechanisms are unknown.

Aerolysin is a pore-forming toxin secreted by *Aeromonas*

hydrophila and is distinct from CDCs. It is produced as an inactive precursor, binds to glycosylphosphatidylinositol-anchored proteins on host cell surfaces, and is proteolytically cleaved. In its mature form, the toxin heptamerizes into a circular ring which forms small pores (1 to 2 nm) permeable to ions but not to proteins (1). K+ efflux through aerolysin pores has been shown to activate the lipid metabolic pathway and the inflammasome (10).

The inflammasome is an important host immunity sensor of invading pathogens. It is a cytosolic protein complex composed of at least a sensor NOD-like receptor, an adaptor protein, and the central effector, caspase-1, a protease which processes proinflammatory cytokines (interleukin-1β [IL-1β] and IL-18) for secretion. The inflammasome senses a variety of intracellular signals such as viruses, type III/IV secreted effectors, intracellular bacteria, various danger signals, and K+ efflux (reviewed in references 6, 18, and 20). *L. monocytogenes* activates the inflammasome; however, the mechanism by which this occurs remains unclear (17, 19, 25).

Here, we show that LLO and other CDCs induce K+ efflux through pore formation at the cell membrane. Furthermore, we demonstrate that this efflux is the signal sensed by the host cell leading to dephosphorylation of H3 (dePH3) and inflammasome activation during infection by *L. monocytogenes*.

MATERIALS AND METHODS

Cell culture and infection. HeLa cells were grown in minimum essential medium, and THP1 cells were grown in RPMI medium with GlutaMAX (GIBCO), 10% fetal calf serum, essential amino acids, and sodium pyruvate. At 24 h before treatment/infection, THP1 cells were differentiated with 0.5 μM phorbol myristate acetate. *L. monocytogenes* was grown in brain heart infusion medium (Difco) at 37°C. Activation of THP1 cells was performed by incubating cells with 1 μg/ml lipopolysaccharide (LPS) for 75 min. Bacteria in exponential phase (optical density [OD] at 600 nm of 1) were used at a multiplicity of infection of 50. The strains used in this study were BUG 600 (wild-type *L. monocytogenes* EGD) and BUG 2132 (Δ*hly* mutant constructed using the pMAD plasmid [3]).

Immunoblotting. Total cell lysates were collected as previously described (11). The antibodies used in this study were against pS10H3 (04-817; Millipore) and

actin (A5441; Sigma). Immunoblot assays were revealed and quantified using a G:Box Gel documentation system (Syngene). Protein levels were normalized to actin.

LLO, perfringolysin (PFO), pneumolysin (PLY), cholesterol pretreatment, and antibody neutralization. His-tagged LLO and mutant forms were purified as described in reference 27. PFO and PLY were used at the same hemolytic titer as LLO (200 ng/ml and 1 μg/ml, respectively). Cholesterol (water soluble, C4951; Sigma) pretreatment was performed for 30 min at 4°C. Neutralizing antibody A4-8 (1 mg/ml) was incubated with LLO for 30 min at 4°C.

K⁺ efflux. PBFI-AM (Molecular Probes) dye was used at 5 μM and incubated for 1 h prior to infection/treatment. Detection of PBFI fluorescence was done on an LSR1 and an ARIAII fluorescence-activated cell sorter (FACS) and then analyzed with FlowJo software. Valinomycin was used at 1 μM for 3 h. High-K⁺ medium contains 135 mM KCl.

Caspase-1 activity. A fluorochrome inhibitor of caspases (FLICA) apoptosis detection kit (Immunochemistry Technologies) for caspase-1 (6-carboxyfluorescein [FAM]-YVAD-FMK) was used according to the manufacturer's instructions. Detection of fluorescence was done using a FACScalibur and analyzed with FlowJo software. YVAD-CHO (Calbiochem) was used at 0.4 μg/ml for 1 h.

IL-1β detection. An enzyme-linked immunosorbent assay (ELISA) for IL-1β was performed using the DuoSet system for human IL-1β (R&D Systems) according to the manufacturer's instructions. THP1 supernatants were diluted 1:10 to 1:50. The color reaction was read at 450 nm using an MRXELISA microplate reader (DYNEX).

Lactate dehydrogenase (LDH) release assay. Measurements of LDH release were performed on the supernatant of HeLa cells. The assay was performed using the Cytotox 96 kit (Promega). Absorbance readings were obtained at 485 nm using a Tristar LB 941 (Berthold). Results were calculated using the formula (OD sample − OD water control)/(OD total lysis − OD water control) × 100.

Statistical analysis of data. P values were calculated by comparing samples two by two to the control sample, unless otherwise indicated by a bracket, and using a standard t test. P values of <0.01 are indicated by ∗∗, and those of <0.08 are indicated by ∗.

RESULTS

Aerolysin induces dePH3. Cells treated with a sublytic concentration of LLO (6 nM for 20 min) show a dramatic dePH3; therefore, we investigated whether aerolysin also acts on host histones. As shown in Fig. 1A, aerolysin decreased the cellular level of phosphorylated H3 on serine 10 (pS10H3) in a dose-dependent manner. Furthermore, as shown in Fig. 1B, at the concentrations used for LLO, aerolysin induced the same 2.5-fold decrease in pS10H3 as LLO. The unexpected result that aerolysin induced a decrease in pS10H3 similar to that caused by LLO suggested that the two toxins use a similar mechanism.

LLO pores cause K⁺ efflux from the host cytoplasm. We hypothesized that the only feature common to aerolysin and LLO that could lead to dePH3 was their capacity to induce ion permeability through plasma membrane pores. Indeed, calcium influx and potassium efflux have been shown to occur upon pore formation by aerolysin (4, 10). We had shown that chelating extracellular Ca^{2+}, thereby blocking its influx into cells, had no effect on LLO-induced dePH3 (11). We hypothesized that K⁺ efflux, although not previously described during an *L. monocytogenes* infection, might be the trigger for histone modification. We thus investigated whether K⁺ efflux was indeed occurring upon infection by *L. monocytogenes*. To measure K⁺ efflux, we used a fluorescent, membrane-permeant, and selective indicator of K⁺ concentration, PBFI. As the concentration of K⁺ is higher inside than outside cells, cells incubated with PBFI became fluorescent (Fig. 2A). A decrease in PBFI fluorescence is observed upon K⁺ efflux, as shown with the control for a potassium ionophore, valinomycin (Fig. 2B). With this method, we evaluated PBFI fluorescence in THP-1 and HeLa cells infected with wild-type *L. monocytogenes* at a
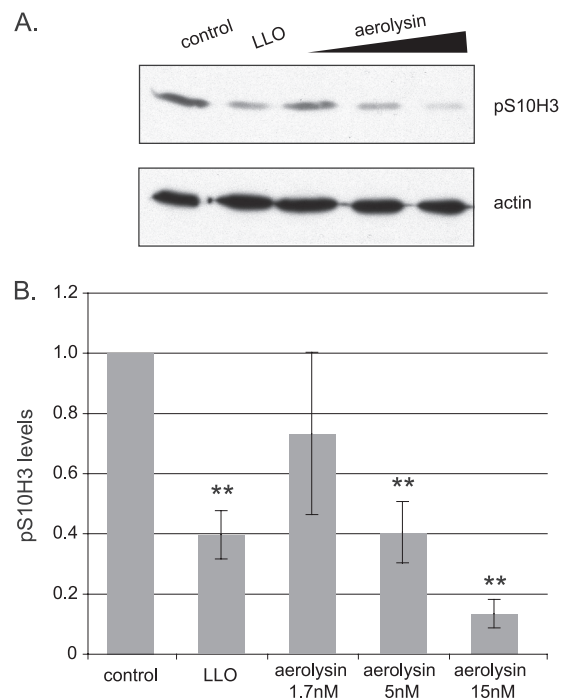

FIG. 1. Aerolysin induces dePH3. (A) Representative Western blot assay of HeLa cells treated with LLO (6 nM) or aerolysin (1.7, 5, or 15 nM) for 20 min. Actin was used as a loading control. (B) Quantification of Western blots. All data are normalized to the control sample. Error bars show the standard error of the mean calculated for at least 3 experiments.

multiplicity of infection of 50 (Fig. 2A). It should be noted that PBF1 fluorescence was measured only in the population of cells that were alive (as determined by the forward/side scatter [FSC/SSC] plot), which represents at least 90% of the cells (data not shown). Figure 2A shows that at 1 h 30 min postinfection, the levels of PBFI fluorescence decreased significantly, demonstrating that K⁺ efflux was occurring. In contrast, upon infection with a mutant with a deletion of the gene encoding LLO (Δ*hly* mutant), no PBFI fluorescence was lost, suggesting that LLO is necessary for K⁺ efflux. To test whether LLO pores on the plasma membrane (as opposed to pores formed from inside the cell once bacteria have entered) were responsible for the observed K⁺ efflux, bacterial entry was blocked with cytochalasin D and PBFI fluorescence was evaluated. As shown in Fig. 2A, PBFI fluorescence decreased in a similar manner upon infection of cytochalasin D-treated and untreated cells. Therefore, bacterial entry is not necessary for K⁺ efflux, suggesting that LLO secreted by extracellular bacteria, which forms pores in the plasma membrane, may induce K⁺ efflux.

To determine whether the K⁺ efflux observed during infection was occurring through LLO pores at the plasma membrane, we measured the PBFI fluorescence of HeLa cells treated exogenously with various concentrations of purified LLO. As shown in Fig. 2B, PBFI fluorescence decreased in a dose-dependent manner upon the addition of LLO. To correlate the loss of PBFI fluorescence in LLO-treated cells with pore formation, we measured propidium iodide (PI) staining under the same conditions. Indeed, upon cell permeabilization, PI enters and stains DNA,
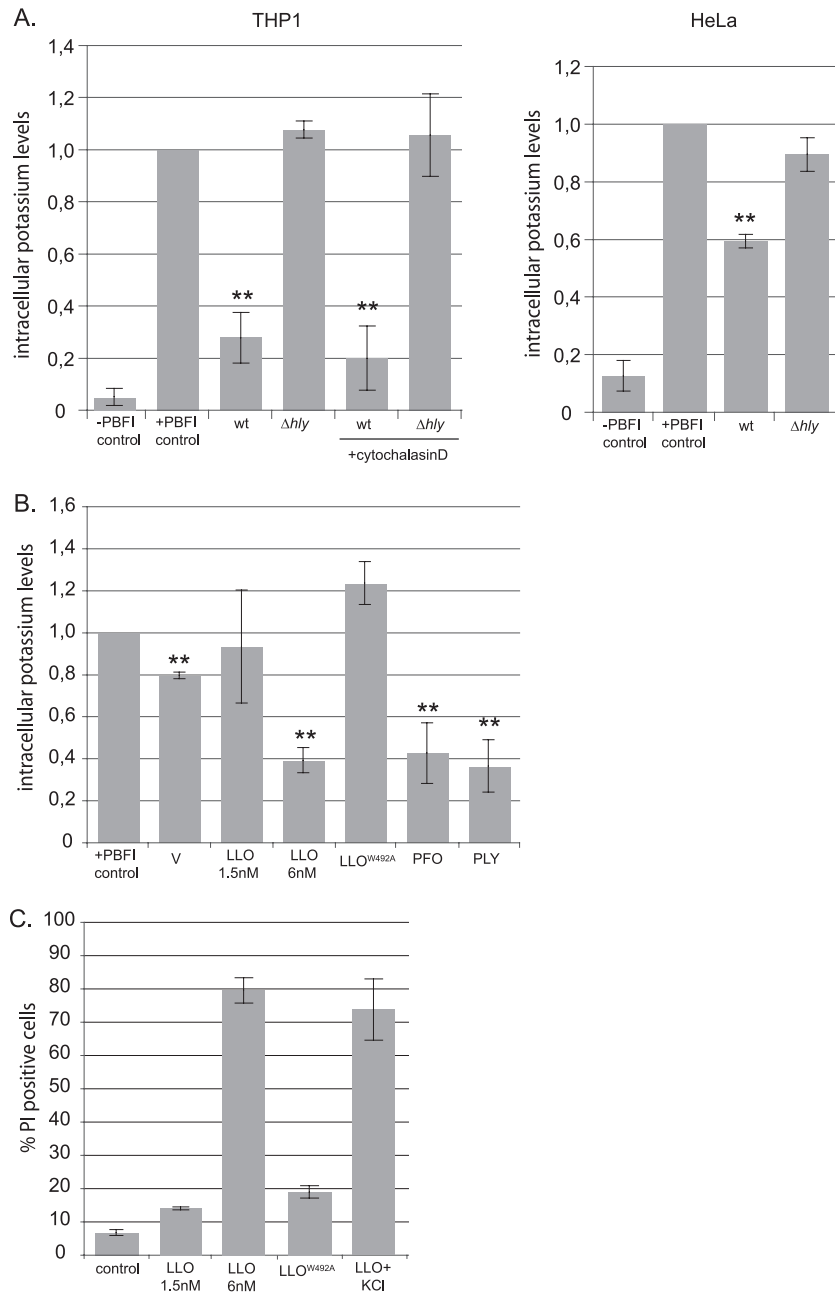
FIG. 2. *L. monocytogenes* induces K$^+$ efflux during infection. (A) THP1 and HeLa cells are marked with PBFI. Data represent the geometric mean PBFI fluorescence normalized to that of the +PBFI control sample, as measured by FACS analysis. Cells were infected at a multiplicity of infection of 50 for 1 h 30 min. Cytochalasin D pretreatment was performed for 30 min prior to infection. (B) HeLa cells marked with PBFI were treated with valinomycin (V) or purified CDC toxins, as indicated on the histogram. Data represent the geometric mean PBFI fluorescence normalized to the +PBFI control sample, as measured by FACS analysis. (C) HeLa cells were stained with PI. Data represent the percentage of PI fluorescent cells as determined by FACS analysis. Error bars are the standard error of the mean calculated for at least 3 experiments (10,000 cells were measured during each experiment). wt, wild type.

which is then detected by FACS analysis. As for the PBFI fluorescence, PI fluorescence was measured only in the population of cells that were alive, as determined by the FSC/SSC plot (data not shown). Figure 2C shows that PI staining increased in a dose-dependent manner upon treatment with LLO, and therefore, the observed decrease in PBFI fluorescence correlates with pore formation.

To show that K$^+$ efflux was dependent on pore formation, we used an LLO variant bearing a W-A replacement at amino acid 492 that binds to host membranes without forming pores (22). We verified that this mutant, used at the same concentration as wild-type LLO, was not forming pores by PI staining (Fig. 2C). When we measured the levels of PBFI after treatment with LLO^{W492A}, the fluorescence detected was similar to

that in untreated cells (Fig. 2B), showing that pore formation is required for K⁺ efflux.

Interestingly, HeLa cells treated with two other CDC toxins, PFO, secreted by *Clostridium perfringens*, and PLY, secreted by *Streptococcus pneumoniae*, also showed a significant reduction in PBFI fluorescence (Fig. 2B). Therefore, K⁺ efflux is a common feature induced by pore-forming toxins secreted by unrelated bacteria.

K⁺ efflux is not blocked by cholesterol treatment of LLO. It has been reported that LLO pore formation can be blocked by preincubating the toxin with cholesterol, which is hypothesized to prevent pore formation without compromising membrane binding, through an unknown mechanism (13). In fact, we had previously shown that preincubation of LLO with cholesterol prior to cell treatment blocked LDH release, suggesting that pore formation was inhibited (11). Using this technique, we tried to block potassium efflux by preincubating LLO with cholesterol. Two concentrations of cholesterol were used to incubate with LLO, 1 and 100 μM, the higher one representing a 15-fold molar excess of cholesterol compared to LLO. Using an LDH release assay, we verified that those concentrations of cholesterol were in fact blocking pore formation, as shown in Fig. 3A. In Fig. 3B, the same preincubation of LLO with cholesterol was performed as in Fig. 3A, but we measured potassium efflux from cells rather than LDH release. Unexpectedly, we observed that the PBFI fluorescence of cells treated with LLO/cholesterol is as low as that of cells treated with LLO alone. This suggests that ion-permeable pores are still formed under these conditions. To determine whether cells are indeed permeabilized, we measured PI fluorescence upon treatment with LLO/cholesterol (Fig. 3C). We observe that the levels of PI fluorescence of cells treated with LLO/cholesterol are the same as those of cells treated with LLO alone, suggesting that the same amount of permeabilization is occurring under both conditions. To verify that the LLO preparation was pure, we neutralized LLO with a specific antibody (A4-8) previously shown to inhibit LLO binding (23). As shown in Fig. 3C, this neutralization blocked PI entry into cells and therefore demonstrated that no other factor besides LLO was responsible for pore formation in our LLO preparation. Together, these data show that small pores permeable to ions and PI are still formed upon incubation with cholesterol-pretreated LLO, whereas large pores permeable to LDH are not.

LLO-dependent K⁺ efflux is required for dePH3. Having established that K⁺ efflux was occurring through LLO pores, we investigated whether it was necessary for LLO-induced dePH3. We measured levels of pS10H3 by Western blot assay under conditions where K⁺ efflux was blocked. K⁺ efflux can be blocked by incubating cells in medium containing high concentrations of K⁺ (10). We first verified that high-K⁺ medium was not inhibiting LLO's pore formation ability by measuring PI staining. Figure 2C shows that cells treated with LLO in regular medium demonstrate a PI staining similar to that of cells incubated in high-K⁺ medium, and therefore increasing the concentration of K⁺ in the medium does not block LLO's pore-forming ability. However, if we measure the levels of pS10H3 (Fig. 4) in cells treated with LLO under conditions of high extracellular K⁺, they do not decrease as they do in regular medium. This indicates that inhibition of K⁺ efflux blocks LLO-dependent dePH3. We also verified that blocking a
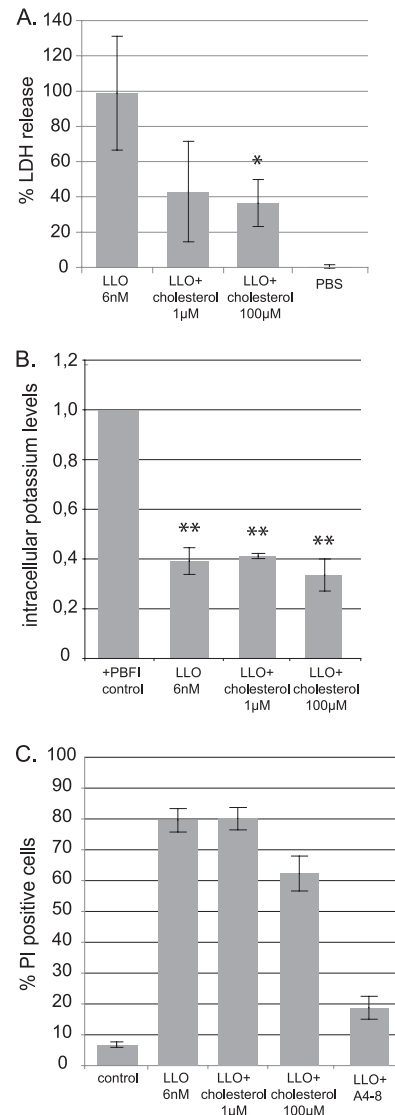

FIG. 3. Cholesterol pretreatment of LLO does not fully block pore formation. (A) LDH release assay performed with HeLa cells. LLO was preincubated with the indicated concentrations of water-soluble cholesterol prior to the addition to cells. Percentages were calculated relative to the LDH released by cells lysed with detergent. (B) HeLa cells are marked with PBFI. Data represent the geometric mean PBFI fluorescence normalized to that of the untreated sample, as measured by FACS analysis. (C) HeLa cells were stained with PI. LLO was preincubated either with cholesterol or with neutralizing A4-8 antibody prior to addition to cells. Data represent the percentage of PI fluorescent cells as determined by FACS analysis. Error bars are the standard error of the mean calculated for at least 3 experiments (10,000 cells were measured during each FACS experiment).

calcium influx by using EGTA did not block LLO-induced dePH3, suggesting specificity to potassium. To determine whether binding of LLO to the membrane, rather than pore formation, is the required step for dePH3, we treated cells with LLO^W492A, which does not induce K⁺ efflux or pore formation (Fig. 2B and C). Figure 4 shows that upon treatment with LLO^W492A, there was no decrease in pS10H3, and therefore K⁺ efflux through LLO formed pores is the signal inducing dePH3.
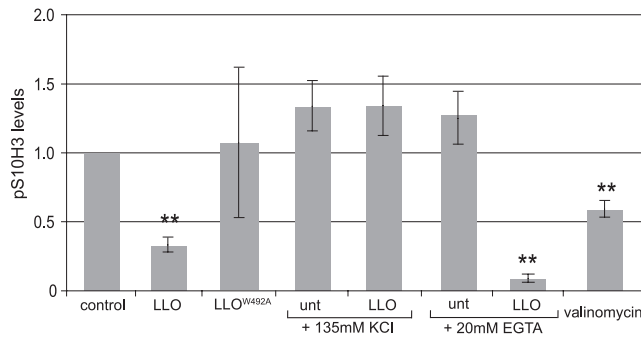
FIG. 4. K$^+$ efflux leads to dePH3. HeLa cells were treated with LLO, LLO^{W492A}, or valinomycin, and the cell medium contained either K$^+$ or EGTA where indicated. Data represent the quantification of Western blots. Error bars are the standard error of the mean calculated for at least 3 experiments. unt, untreated.

Conversely, we measured the levels of pS10H3 under conditions where a specific K$^+$ efflux was generated using an ionophore, valinomycin. As shown in Fig. 2B by PBFI staining, incubation of cells with valinomycin does, in fact, induce a small but significant K$^+$ efflux (a vehicle control for valinomycin treatment, dimethyl sulfoxide [DMSO], was tested and had no effect on pS10H3 levels [data not shown]). Concomitant with this K$^+$ efflux, we observe that valinomycin is also able to induce a small but significant decrease in pS10H3 (Fig. 4). Therefore, K$^+$ efflux is both necessary for LLO-induced dePH3 and sufficient to induce dePH3.

LLO-dependent pores are required for caspase-1 activation and IL-1β release. Since K$^+$ efflux has been shown to be one of the major signals activating the inflammasome, we investigated whether this was the case during an *L. monocytogenes* infection. We first measured caspase-1 activity with a fluorescently labeled inhibitor (FAM-FLICA) (10). As shown in Fig. 5A, infection with wild-type *L. monocytogenes*, but not an Δ*hly* mutant, led to an increase in the percentage of FAM-FLICA fluorescent cells, indicative of caspase-1 activation. To verify that caspase-1 was becoming active due to extracellularly produced LLO, bacterial entry was blocked using cytochalasin D. Upon the infection of cells under these conditions, the percentage of FAM-FLICA fluorescent cells was similar to that of treated cells, suggesting that caspase-1 activation is triggered by extracellular LLO. We then used purified LLO to determine whether LLO was sufficient for caspase-1 activation and measured the percentage of FAM-FLICA fluorescent cells. As shown in Fig. 5A, most of the cell population activated caspase-1 upon incubation with LLO. We then investigated whether caspase-1 activation depended on K$^+$ efflux through LLO pores. We first treated cells with the mutant LLO^{W492A} and showed that there was no significant increase in FAM-FLICA fluorescent cells and therefore no caspase-1 activation (Fig. 5A). Furthermore, upon the blocking of K$^+$ efflux by incubation of cells in high-K$^+$ medium and treatment with LLO, the percentage of cells activating caspase-1 dropped significantly. Taken together, these results indicate that K$^+$ efflux through LLO pores leads to caspase-1 activation.

The second method by which we measured caspase-1 activation is evaluation of the level of a caspase-1 product, IL-1β. ELISAs were performed with supernatants of THP1 cells in-
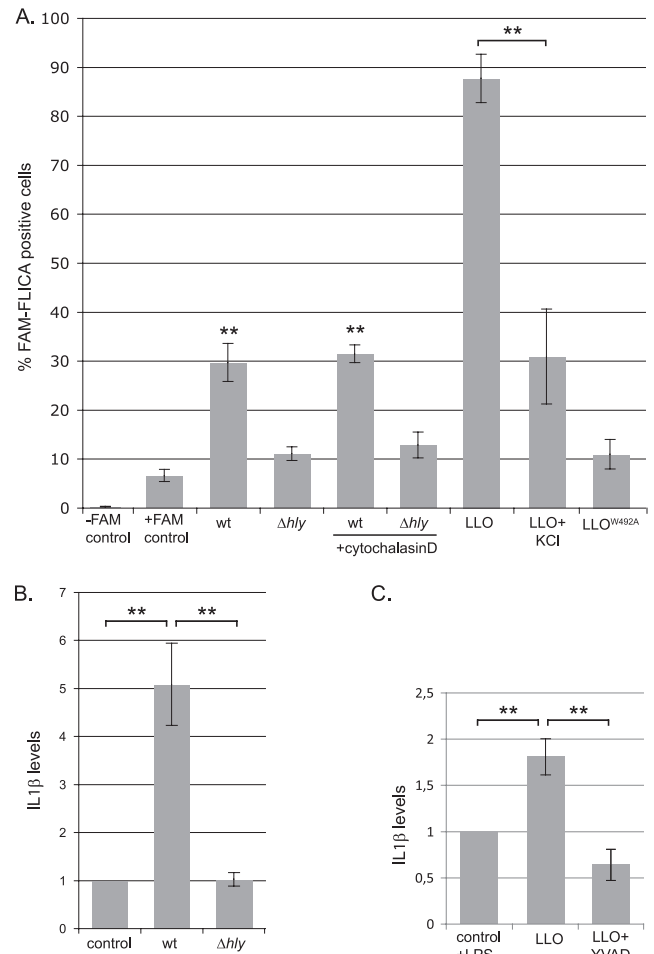

FIG. 5. K$^+$ efflux induces inflammasome activation. (A) HeLa cells were marked with FAM-FLICA and infected with *L. monocytogenes* at a multiplicity of infection of 50 for 1 h 30 min or treated with purified LLO or LLO^{W492A}. Cytochalasin D pretreatment was performed for 30 min prior to infection. Data represent the percentage of FAM-FLICA fluorescent cells as determined by FACS analysis. (B) IL-1-β ELISA performed on the supernatant of THP1 cells infected with *L. monocytogenes* at a multiplicity of infection of 50 for 1 h 30 min. Values are normalized to the control sample. (C) IL-1-β ELISA performed on the supernatant of activated THP1 cells (LPS pretreated) incubated with purified LLO or YVAD and LLO. Error bars are the standard error of the mean calculated for at least 3 experiments (10,000 cells were measured during each experiment). wt, wild type.

fected with *L. monocytogenes* for 1 h 30 min. Figure 5B shows that IL-1β levels rose 5-fold upon infection with wild-type bacteria. However, upon infection with an Δ*hly* mutant, no IL-1β was produced, showing that LLO is necessary for this production.

To demonstrate that LLO is activating caspase-1 and therefore IL-1β production, we treated LPS-activated cells with purified LLO. Indeed, the pro-IL-1β cytokine is not constitutively expressed and requires transcriptional induction by LPS, for example. Upon the production of pro-IL-1β, activated caspase-1 can catalyze its cleavage into the secreted and active form of IL-1β. Figure 5C shows that a significant level of IL-1β is produced in LPS-activated cells treated with LLO. To verify that the IL-1β produced under these conditions was due to
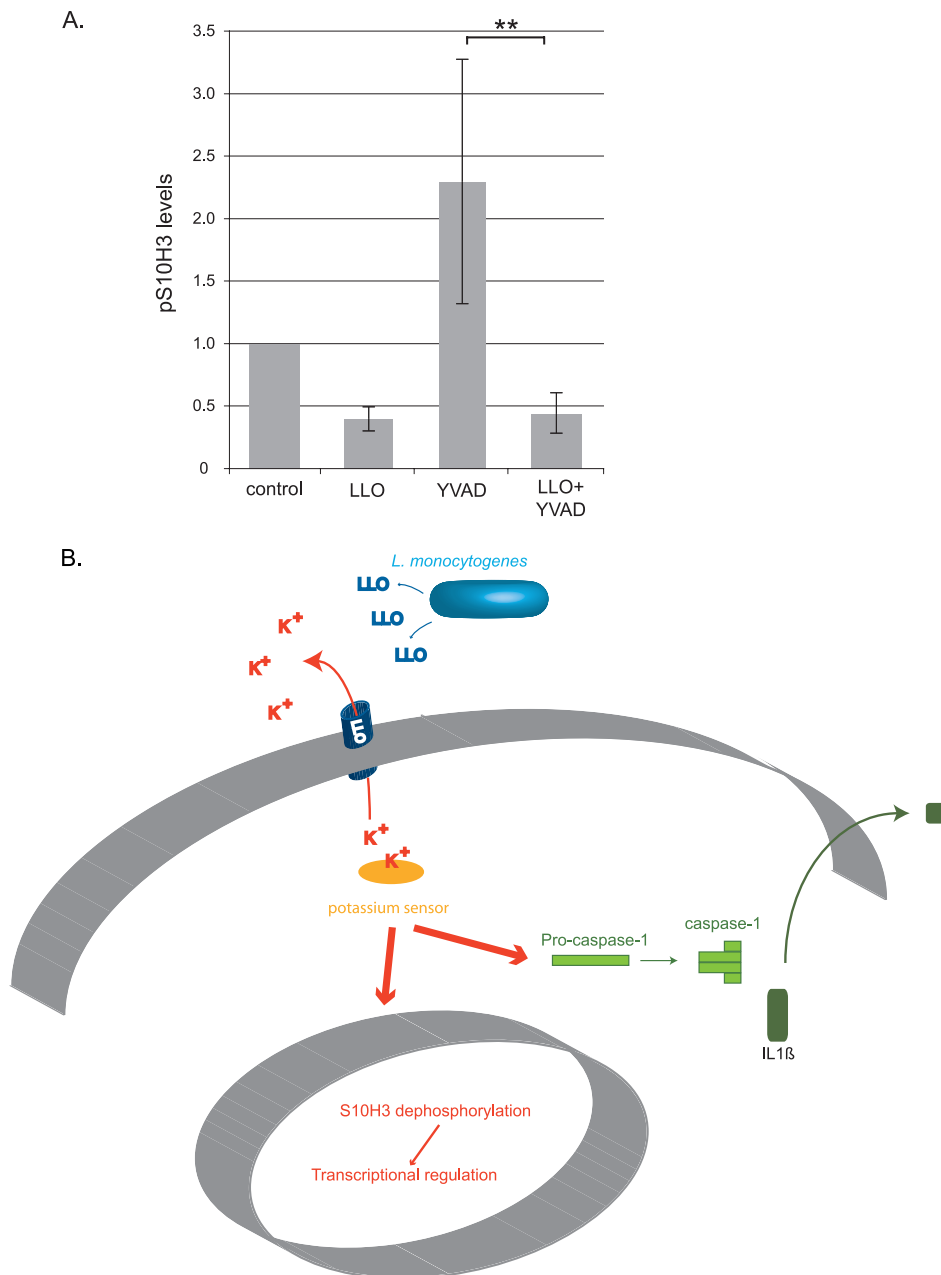
A.

B.

FIG. 6. dePH3 and inflammasome activation are two separate pathways. (A) HeLa cells were treated with either purified LLO or YVAD and LLO. Data represent the quantification of Western blots. Error bars are the standard error of the mean calculated for at least 3 experiments. (B) Model showing that *L. monocytogenes* modulates host histones and activates the inflammasome, two separate pathways initiated by K^+ efflux through LLO-formed pores. Our results suggest that an intracellular receptor responds to K^+ levels and initiates the appropriate downstream response, thereby conferring specificity to the response.

caspase-1 activation, cells were pretreated with the specific caspase-1 inhibitor YVAD. As shown in Fig. 5C, IL-1β production is blocked upon the incubation of cells with LLO and YVAD. Taken together, these results show that LLO from the extracellular milieu can activate the inflammasome prior to bacterial entry.

dePH3 and inflammasome activation are two separate pathways. Since potassium efflux through LLO pores is necessary for dePH3 and is responsible for activating caspase-1, we hypothesized that caspase-1 activation may have a role in dePH3.

To determine whether this was the case, we treated cells with the caspase-1 inhibitor YVAD. Figure 5C shows that this inhibitor is active, as it entirely blocks IL-1β production by LLO. As shown in Fig. 6, we measured the levels of pS10H3 in cells treated with the caspase-1 inhibitor (a vehicle control for YVAD treatment, DMSO, was tested and had no effect on pS10H3 levels [data not shown]). We observed the same dePH3 in YVAD-treated cells as in nontreated cells. Furthermore, although we show that LLO induces caspase-1 activation and IL-1β release from THP-1 cells, we have never observed

dePH3 in this cell line (data not shown). Thus, caspase-1 activation does not correlate with dePH3.

DISCUSSION

In this study, we have unveiled a signaling cascade activated by several bacteria during infection that links K$^+$ efflux to dePH3. We had previously shown that LLO and other CDC toxins induce dePH3 but had not identified the underlying mechanism (11). Here, we first showed that aerolysin, which is known to induce K$^+$ efflux, also dephosphorylates H3. We then demonstrated that LLO pores are also permeable to K$^+$ ions and that blocking either pore formation or K$^+$ efflux abrogated LLO-dependent dePH3. We have also demonstrated that LLO-induced K$^+$ efflux is a signal activating the inflammasome during *L. monocytogenes* infection and that this cascade is unlinked to dePH3. Therefore, K$^+$ efflux is a potent signal, induced by different bacteria during infection, which triggers at least two separate pathways (see model in Fig. 6B).

Our results unexpectedly show that aerolysin and CDCs, which have distinct modes of action and, most importantly, form different-size pores, have the same effect on phosphorylated H3. We had previously reported that cells treated with LLO (6 nM for 20 min) modulate the transcription of approximately 200 genes that correlated with changes in modified histones at their promoter (11). Thus, only a specific subset of genes shows histone modifications. That aerolysin also induces dePH3 through a K$^+$ efflux-dependent mechanism could suggest that a similar transcriptional response would be imposed. Interestingly, the genes identified as modulated upon aerolysin treatment were not modulated upon LLO treatment (10), suggesting that a level of specificity exists, although its basis is unknown. Furthermore, although K$^+$ efflux is sufficient to trigger dePH3, the decrease observed upon valinomycin treatment is not as important as that obtained upon LLO treatment, suggesting that LLO may use another factor to trigger a full response. Therefore, although K$^+$ efflux can be generated under different conditions, the effects on histone H3 are not the same for all conditions, and specificity appears to be imposed by unidentified factors.

Interestingly, K$^+$ efflux has not been previously linked to histone modifications. We hypothesize that similarly to Ca^{2+} signaling, an intracellular K$^+$ sensor/receptor is probably involved in histone modifications (see model in Fig. 6B). Of note, the crystal structures of several histone deacetylases identified a K$^+$ ion in their structure (5, 31). Furthermore, K$^+$ regulates the activity of histone deacetylase 8, rendering this enzyme's activity sensitive to changes in the cellular K$^+$ concentration (8). Interestingly, we have shown that LLO-mediated dePH3 correlates with a deacetylation of histone H4, and therefore, the two events could be linked (11). Therefore, histone deacetylases, which modify many intracellular proteins, might be important K$^+$ sensors.

Our results show that LLO-induced K$^+$ efflux is a signal that contributes to inflammasome activation during infection with *L. monocytogenes*. It has been suggested that LLO activation of caspase-1 is due to bacterial release from the vacuole exposing the bacteria to intracellular sensors of the inflammasome (7, 21, 32). However, we show here that the inflammasome may be activated prior to listerial invasion of cells, through LLO pore formation at the plasma membrane and K$^+$ efflux. Our findings could explain conflicting published findings on which inflammasome sensor, NLP3 or AIM2, is involved in responding to *L. monocytogenes* (7, 19, 21). Indeed, in light of what we show here, we propose that several waves of inflammasome activation occur, depending on the signal sensed. Extracellular *L. monocytogenes* secreting LLO would activate the NLP3 inflammasome (a sensor of membrane damage), and once bacteria have reached the host cytosol, the AIM2 inflammasome would be solicited (a sensor of foreign DNA). The implications of such a hypothesis are 2-fold. First, since LLO is a secreted and diffusible factor, a large number of cells may sense and respond to the "LLO signal," compared to cells that are infected with *L. monocytogenes*. Second, cells that are responding only to the extracellular "LLO signal" might exhibit a different immune response than those infected with intracellular bacteria.

In this study, we have reinforced two important aspects of LLO's mechanism of action which are still poorly documented and understood. First, we demonstrate that inflammasome activation and histone modifications occur through the action of LLO on the plasma membrane. Although studies have shown that LLO's maximal activity occurs at acidic pH, which are the conditions found inside the internalization vacuole (29), we clearly see pore formation activity during infection prior to bacterial invasion or with purified LLO added to the culture supernatant. In agreement with these observations, many reports show the activity of LLO from the outside the cell (15, 16, 26, 27), suggesting that LLO acts in a manner similar to that of other CDCs secreted by extracellular bacteria. Second, we show that the commonly used method of preincubating LLO with cholesterol to block pore formation does not prevent the formation of small ion-permeable pores. We do see that large pores, such as those that release LDH, are blocked by this technique; however, we show here that small pores, such as those permeable to ions, are still formed. We observe that this is the case even if we use a saturating amount of cholesterol (15-fold molar excess compared to LLO). In fact, small pores have been observed in the membrane of *L. monocytogenes*-containing vacuoles (30). What cholesterol is doing at the molecular level to limit the action of LLO remains unknown and should be considered as inhibiting only large pores.

In conclusion, our results define K$^+$ efflux as occurring during infection with *L. monocytogenes* and as a signal leading to caspase-1 activation and dePH3. As schematically represented in Fig. 6B, histone modifications and inflammasome activation, because caspase-1 is not required for dePH3, are two independent pathways. Since none of the components of the inflammasome have been shown to have a link with histone modifications, it is unlikely, although not completely ruled out, that other inflammasome components besides caspase-1 are involved in histone modifications. What arises from our data, as shown in our model, is that a certain degree of specificity must occur in the host cell in response to K$^+$ efflux; this specificity could be conferred by an intracellular K$^+$ sensor. We highlight here a novel signaling cascade triggered by K$^+$ efflux and leading to histone modifications whose cellular components contributing to specificity remain to be uncovered.

REFERENCES

1. **Abrami, L., M. Fivaz, and F. G. van der Goot.** 2000. Adventures of a pore-forming toxin at the target cell surface. Trends Microbiol. **8:**168–172.
2. **Arbibe, L.** 2008. Immune subversion by chromatin manipulation: a 'new face' of host-bacterial pathogen interaction. Cell. Microbiol. **10:**1582–1590.
3. **Arnaud, M., A. Chastanet, and M. Debarbouille.** 2004. New vector for efficient allelic replacement in naturally nontransformable, low-GC-content, gram-positive bacteria. Appl. Environ. Microbiol. **70:**6887–6891.
4. **Bischofberger, M., M. R. Gonzalez, and F. G. van der Goot.** 2009. Membrane injury by pore-forming proteins. Curr. Opin. Cell Biol. **21:**589–595.
5. **Bottomley, M. J., et al.** 2008. Structural and functional analysis of the human HDAC4 catalytic domain reveals a regulatory structural zinc-binding domain. J. Biol. Chem. **283:**26694–26704.
6. **Franchi, L., T. Eigenbrod, R. Munoz-Planillo, and G. Nunez.** 2009. The inflammasome: a caspase-1-activation platform that regulates immune responses and disease pathogenesis. Nat. Immunol. **10:**241–247.
7. **Franchi, L., T. D. Kanneganti, G. R. Dubyak, and G. Nunez.** 2007. Differential requirement of P2X7 receptor and intracellular K$^+$ for caspase-1 activation induced by intracellular and extracellular bacteria. J. Biol. Chem. **282:**18810–18818.
8. **Gantt, S. L., C. G. Joseph, and C. A. Fierke.** 2010. Activation and inhibition of histone deacetylase 8 by monovalent cations. J. Biol. Chem. **285:**6036–6043.
9. **Giddings, K. S., J. Zhao, P. J. Sims, and R. K. Tweten.** 2004. Human CD59 is a receptor for the cholesterol-dependent cytolysin intermedilysin. Nat. Struct. Mol. Biol. **11:**1173–1178.
10. **Gurcel, L., L. Abrami, S. Girardin, J. Tschopp, and F. G. van der Goot.** 2006. Caspase-1 activation of lipid metabolic pathways in response to bacterial pore-forming toxins promotes cell survival. Cell **126:**1135–1145.
11. **Hamon, M. A., et al.** 2007. Histone modifications induced by a family of bacterial toxins. Proc. Natl. Acad. Sci. U. S. A. **104:**13467–13472.
12. **Hamon, M. A., and P. Cossart.** 2008. Histone modifications and chromatin remodeling during bacterial infections. Cell Host Microbe **4:**100–109.
13. **Jacobs, T., et al.** 1998. Listeriolysin O: cholesterol inhibits cytolysis but not binding to cellular membranes. Mol. Microbiol. **28:**1081–1089.
14. **Kayal, S., and A. Charbit.** 2006. Listeriolysin O: a key protein of Listeria monocytogenes with multiple functions. FEMS Microbiol. Rev. **30:**514–529.
15. **Kayal, S., et al.** 2002. Listeriolysin O secreted by Listeria monocytogenes induces NF-kappaB signalling by activating the IkappaB kinase complex. Mol. Microbiol. **44:**1407–1419.
16. **Kayal, S., et al.** 1999. Listeriolysin O-dependent activation of endothelial cells during infection with Listeria monocytogenes: activation of NF-kappa B and upregulation of adhesion molecules and chemokines. Mol. Microbiol. **31:**1709–1722.
17. **Kim, S., et al.** 2010. Listeria monocytogenes is sensed by the NLRP3 and AIM2 inflammasome. Eur. J. Immunol. **40:**1545–1551.
18. **Mariathasan, S., and D. M. Monack.** 2007. Inflammasome adaptors and sensors: intracellular regulators of infection and inflammation. Nat. Rev. Immunol. **7:**31–40.
19. **Mariathasan, S., et al.** 2006. Cryopyrin activates the inflammasome in response to toxins and ATP. Nature **440:**228–232.
20. **Martinon, F., and J. Tschopp.** 2007. Inflammatory caspases and inflammasomes: master switches of inflammation. Cell Death Differ. **14:**10–22.
21. **Meixenberger, K., et al.** 2010. Listeria monocytogenes-infected human peripheral blood mononuclear cells produce IL-1beta, depending on listeriolysin O and NLRP3. J. Immunol. **184:**922–930.
22. **Michel, E., K. A. Reich, R. Favier, P. Berche, and P. Cossart.** 1990. Attenuated mutants of the intracellular bacterium Listeria monocytogenes obtained by single amino acid substitutions in listeriolysin O. Mol. Microbiol. **4:**2167–2178.
23. **Nato, F., et al.** 1991. Production and characterization of neutralizing and nonneutralizing monoclonal antibodies against listeriolysin O. Infect. Immun. **59:**4641–4646.
24. **Palmer, M.** 2001. The family of thiol-activated, cholesterol-binding cytolysins. Toxicon **39:**1681–1689.
25. **Rathinam, V. A., et al.** 2010. The AIM2 inflammasome is essential for host defense against cytosolic bacteria and DNA viruses. Nat. Immunol. **11:**395–402.
26. **Ratner, A. J., et al.** 2006. Epithelial cells are sensitive detectors of bacterial pore-forming toxins. J. Biol. Chem. **281:**12994–12998.
27. **Ribet, D., et al.** 2010. Listeria monocytogenes impairs SUMOylation for efficient infection. Nature **464:**1192–1195.
28. **Schnupf, P., and D. A. Portnoy.** 2007. Listeriolysin O: a phagosome-specific lysin. Microbes Infect. **9:**1176–1187.
29. **Schuerch, D. W., E. M. Wilson-Kubalek, and R. K. Tweten.** 2005. Molecular basis of listeriolysin O pH dependence. Proc. Natl. Acad. Sci. U. S. A. **102:**12537–12542.
30. **Shaughnessy, L. M., A. D. Hoppe, K. A. Christensen, and J. A. Swanson.** 2006. Membrane perforations inhibit lysosome fusion by altering pH and calcium in Listeria monocytogenes vacuoles. Cell. Microbiol. **8:**781–792.
31. **Vannini, A., et al.** 2004. Crystal structure of a eukaryotic zinc-dependent histone deacetylase, human HDAC8, complexed with a hydroxamic acid inhibitor. Proc. Natl. Acad. Sci. U. S. A. **101:**15064–15069.
32. **Warren, S. E., D. P. Mao, A. E. Rodriguez, E. A. Miao, and A. Aderem.** 2008. Multiple Nod-like receptors activate caspase-1 during Listeria monocytogenes infection. J. Immunol. **180:**7558–7564.

Editor: J. B. Bliska